

Observed Reductions of Total Solar Irradiance by Biomass-Burning Aerosols in the Brazilian Amazon and Zambian Savanna

J.S. Schafer^{1,3}, T.F. Eck^{2,3}, B.N. Holben³, P. Artaxo⁴, M.A. Yamasoe⁴, A.S. Procopio⁴

¹ Science Systems and Applications, Inc. (SSAI), Lanham, MD 20706

²University of Maryland-Baltimore County, Goddard Earth Sciences and Technology Center

³NASA/Goddard Space Flight Center, Biospheric Sciences Branch, Code 923, Greenbelt, MD 20771

⁴Departamento de Física Aplicada, Instituto de Física da Universidade de São Paulo, Rua do Matão, Travessa R., 187, São Paulo — SP — Brazil CEP 05508-900

Abstract. Several aerosol and solar flux monitoring sites were established in Brazil for the Large Scale Biosphere-Atmosphere Experiment in Amazonia project. CIMEL sunphotometers and collocated pyranometers were employed at two southern Amazonian sites in order to quantify instantaneous reductions of total irradiance due to high aerosol optical thickness (AOT) smoke events (relative to values modeled for background aerosol conditions). Results from the Brazilian sites are presented for 1999 and for comparison, a similar analysis is discussed for data from three south-central African sites during the burning season of 2000.

The relative reductions in total irradiance at the surface resulting from biomass burning aerosol are observed to be substantial at all sites, ranging from 16% for an aerosol optical thickness (500nm) of 1.0 for the Brazilian sites to an average rate of 22% for the African sites. For a solar zenith interval (25-35°), these rates equate to reductions of roughly -145 W/m² and -210 W/m² respectively, for a unit AOT. Instantaneous reductions of 337 W/m² were observed for the heaviest smoke conditions (AOT: ~3.0) in Brazil.

Introduction

Atmospheric aerosols modify climate by direct absorption and scattering of solar energy and indirectly when fine mode aerosols act as auxiliary cloud condensation nuclei (CCN), thereby decreasing average cloud droplet size and enhancing planetary albedo [Facchini et al., 1999]. Additionally, absorbing aerosols may also modify climate by the semi-direct effect [Hansen et al., 1997] wherein heating of the aerosol layer reduces cloud cover by increasing atmospheric stability or by evaporating clouds [Ackerman et al., 2000]. Highly absorbing smoke aerosols, such as are regularly produced in great quantity during the annual biomass-burning season in Amazonia have an effect on the regional radiation budget and climate dramatically larger than that observed in even the most polluted of urban environments.

Global climate models require better quantification of the single scattering albedo of tropical aerosols in the visible spectrum [Toon, 1995] as well as their seasonal and inter-annual variability. Also, the importance of characterizing strong regional sources (e.g., Amazonian fire centers) sufficiently for modeling purposes is widely recognized.

Improved parameterization of biomass burning aerosols is essential for satellite data driven surface radiation models which are known to currently overestimate shortwave (SW) irradiance by poorly accounting for highly-absorbing smoke aerosols. Large discrepancies between measured and modeled SW irradiance of 20-40 W/m² [Wild, 1999] and 40-80 W/m² [Konzelman et al., 1996] have been documented in connection with prevalent savanna fires in Africa, while model overestimations of incoming solar radiation up to 44% are reported for regions of the Brazilian Amazon and Cerrado affected by biomass burning [Pereira et al., 1999].

In this paper we present the data and analysis of aerosol optical thickness (AOT) and total solar fluxes for two Large-Scale Biosphere-Atmosphere Experiment in Amazonia (LBA) sites in the southern Amazon (Abracos Hill: 10.762S, 62.357W; Alta Floresta: 9.872S, 56.104W) for 1999 and 3 sites in southern Zambia (Mongu: 15.25S, 23.15E; Zamezi: 13.52S, 23.1E; Ndola: 12.98S, 28.65E) for 2000. In particular, the analysis focuses on the effects of fire-generated aerosols on surface irradiance and additionally on the retrieval of aerosol absorption information from synthesis of the simultaneous AOT and flux data.

Instrumentation And Sites

To date, eight aerosol monitoring sites, have been established in Brazil for the LBA project as a subset of the AERONET network [Holben et al., 1998]. The first two sites were developed in the states of Rondônia (Abracos Hill) and Mato Grosso (Alta Floresta) in January 1999 and data from these locations were used in this study. Both sites were equipped with a CIMEL sunphotometer and two flux sensors—a Skye-Probetech SKE 510 PAR (photosynthetically-active radiation) Energy sensor (spectral range: 400-700 nm) and a Kipp and Zonen CM-21 pyranometer (305-2800 nm) for measuring the total solar spectrum. The flux sensors record the instantaneous irradiance at 1-minute intervals. The automatic sunphotometers (model CE-318A) were manufactured by CIMEL Electronique and are discussed at length in Holben et al. [1998]. Each is equipped with narrow bandpass filters in the visible and near infrared with center wavelengths at 340, 380, 440, 500, 675, 870, 940, and 1020 nm. The CIMEL sunphotometer provides AOT at each of these wavelengths, except for the 940 channel which is used to derive total column water vapor. In addition to the direct solar irradiance measurements that are made with a field of view of 1.2°, these instruments measure the sky radiance in four spectral bands (440, 670, 870, and 1020

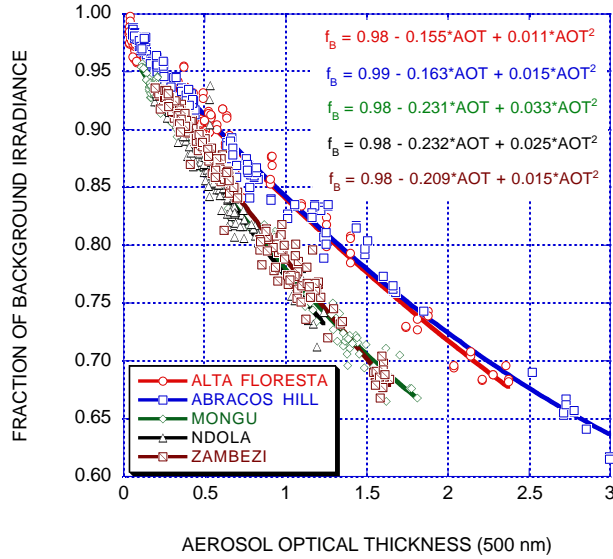


Figure 1a: Fraction of total irradiance observed relative to that expected for background aerosol conditions (SZ: 25-35)

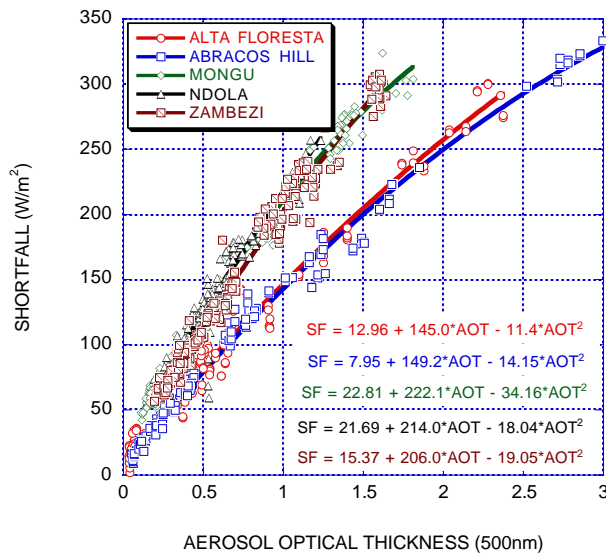


Figure 1b: Shortfall of total irradiance observed relative to that expected for background aerosol conditions (SZ: 25-35)

nm). It is these sky radiance measurements that are used to retrieve additional column aerosol properties including volume size distribution, phase function, real and imaginary component of refractive index, effective radius and single scattering albedo that are routinely computed with the AERONET inversion algorithms [Dubovik and King, 2000].

Calibration factors provided by the manufacturer (Kipp and Zonen) were applied for the pyranometers. Additional confidence was acquired by using in-situ comparisons to a the 6S radiative transfer model on optimal days. The 6S model that was used is based on the successive order of scattering method and is described in Vermote et al. [1997]. Field days used were of minimal aerosol-loading ($\text{AOT } 500\text{nm} < 0.1$) under cloud-free conditions. Such aerosol levels are sufficiently low to render an exact knowledge of the absorption properties unimportant for

AOT (500nm)	Fraction of Background		Shortfall (W/m^2)	
	Brazil avg.	Africa Avg.	Brazil avg.	Africa Avg.
0.5	0.91	0.87	81	121
1.0	0.84	0.78	145	210
2.0	0.72	0.63	254	353
3.0	0.63	----	337	----

Table 1: Observed fraction of background total irradiance and energy shortfall at a range of AOT (500nm) values based on averages for the Brazilian and African sites

computing clear-sky insolation. The difference between measured and modeled irradiance (using measured AOT) for the five sites ranged from 0-2%, in good agreement with the stated accuracy of the manufacturer. The pyranometers have been observed to remain very stable (better than 1%) over the period of deployment.

Analysis

Cloud-screening and Synthesis of Aerosol and Flux Data

Instantaneous pyranometer measurements were screened with a temporal variability filter in an effort to remove observations modified by the proximity of scattered to broken cloud cover. This filter relies on a goodness of fit criterion for the linear regression of measured irradiance on cosine(solar zenith) and thus is primarily effective only at removing observations affected by variable cloud conditions. To reduce the chance of contamination (enhancement) by peripheral clouds, low variability was required for a moving 2-hour window centered on all candidate flux observations, and the central flux value could not deviate significantly from the flux expected from the associated 2 hour regression. The goodness of fit critical value for acceptable variability employed was subjectively chosen to be sensitive enough to detect the temporal signature of typical cumuliform cloud cover without eliminating observations acquired during variable smoke plume sky conditions.

The resulting flux data set then required further cloud-screening to eliminate observations acquired during uniform cloud conditions that might have passed the variability filter. To achieve this, the flux data were matched with concurrent AOT observations (acquired within a ± 1 minute window) from collocated CIMEL sunphotometers that were evaluated as uncontaminated by cloud using the AERONET cloud-screening algorithm (Smirnov et al., 2000). The CIMEL-derived atmospheric parameters of AOT, Angstrom wavelength exponent, and column water vapor were associated with the simultaneous pyranometer measurements and the data were then processed to select cases when the solar zenith angle was between 25 and 35 degrees and the wavelength exponent was greater than 1.0. This procedure was applied to the dry (biomass burning) season data at each of the five sites used in this study. The final matched data sets of pyranometer and corresponding CIMEL measurements contained 165 observations for Alta Floresta (from 40 different days), 193(35) at Abracos Hill, 154(27) at Mongu, 139(29) at Ndola, and 204(31) at Zambezi.

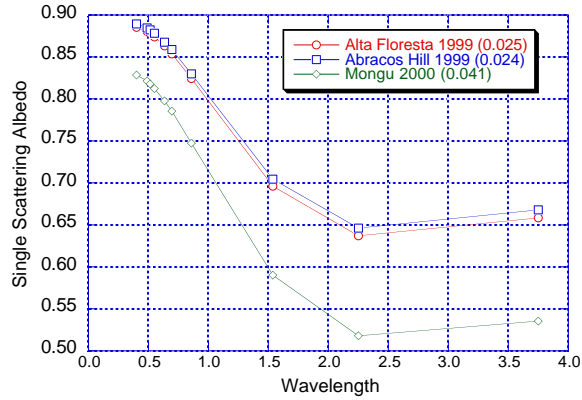


Figure 2: Wavelength dependence of SSA for an imaginary refractive index equal to the average value estimated for each location (as used in model)

For each qualifying 1-minute, instantaneous pyranometer measurement, the ratio (f_B) of the measured flux to the theoretical, clear-sky flux for background aerosol at the relevant solar zenith angle (6S modeled data) was determined.

$$f_B = \frac{\text{IRRADIANCE_}[AOTx;SSAx;WVx]}{\text{IRRADIANCE_}[AOT = 0.04;SSA = 0.97;WVx]}$$

The fluxes for background aerosol condition were modeled using an AOT at 550nm of 0.04, and an imaginary component of refractive index of 0.003, which corresponds to an approximate SSA of 0.97 at 550nm. For each instantaneous flux observation, the expected background flux was computed using the observed column water vapor amount, date, and solar zenith angle, and then the ratio of each instantaneous measurement to the predicted cloudless sky, background value was evaluated. The modeling process used the water vapor amount appropriate to each measurement to minimize the effect of variation in column water vapor upon it and better isolate the aerosol effects on the f_B parameter. In addition, the range of water vapor observed at each site during the interval of study was small (<2 cm) with standard deviations of less than 1 cm.

Single Scattering Albedo Estimation Procedure

Estimates of the effective single scattering albedo (SSA) were also evaluated for the pyranometer observations at the Brazilian sites and at Mongu, Zambia as part of a related modeling process. The single scattering albedo is a measure of the bulk absorption of an aerosol.

The cloud-screened, matched pyranometer data sets were used as input to the 6S model as for the calculation of f_B , except that rather than modeling expected flux for background aerosol conditions, the observed AOT during each flux measurement was an input. Using the appropriate column water vapor, solar zenith angle and day of year for each measurement, the expected flux was computed for a range of imaginary refractive indices (n_i) to determine the trend of total flux for increasingly absorbing aerosols. The refractive indices selected (0.000, 0.009, 0.020, 0.033, 0.046 and 0.061) represent a range of single scattering albedo of approximately 0.75 to 1.0 at 550nm. For each series of 6S model runs, a wavelength-invariant imaginary refractive index was used which is a reasonable assumption for black carbon [Bergstrom et al., 2001]. The derived SSA used by the 6S model

for a given n_i decreases with increasing wavelength. The input aerosol size distribution was based on an average of distributions derived from the set of optimal CIMEL sunphotometer retrievals during the dry season of 1999 at Abracos Hill, Brazil. Since the aerosol volume size distribution changes markedly with smoke aerosol optical thickness, the retrievals were grouped into 15 bins according to AOT value, and the appropriate size distribution was then systematically used in 6S based on the measured AOT. Although the wavelength dependence of SSA has some sensitivity to the size distribution used, the difference in SSA between the aerosol distributions for moderate (AOT 500: 1.0) and heavy (AOT 500: 2.0) smoke conditions is generally 0.01-0.02 over the visible wavelength region. This suggests that employing size distributions derived from Abracos Hill as generalized input (selected by AOT) for the other 2 locations is not likely to introduce significant inaccuracies.

The model outputs both a predicted flux and a single effective SSA that represents the single scattering albedo over the total spectrum weighted by the relative solar signal at each wavelength. A trend line was fit to the resultant modeled fluxes and effective SSA computed for each n_i for each set of observed conditions supplied by the matched flux data set. Instantaneous flux measurements were then used to interpolate the theoretical effective SSA for each observation. The basic principles of this technique are comparable to those employed by Eck et al. in similar studies in Brazil and Africa (Eck et al., 1998, 2000), though the implementation has been modified.

Results

The disparity in both southern Amazonia and south-central Africa between the wet season and dry (biomass-burning) season aerosol regimes is profound. Daily average aerosol optical thickness values (AOT) increase by greater than an order of magnitude in southern Amazonia between the wet and dry season. Predictably, these elevated atmospheric levels of smoke aerosol produce substantial reductions in both photosynthetically active radiation (PAR) [Eck et al., 1998] and total global radiation. At Alta Floresta, one week during a dry season interval of heavy smoke (average AOT 500nm= 1.7) experienced a prolonged reduction of daily integrated PAR insolation of approximately 35% that corresponds to a typical daily shortfall of 3-4 MJ . m⁻² in relation to background aerosol conditions [Schafer et al., submitted to JGR, 2001]. In this study, the instantaneous reductions in total flux were also found to be significant.

The computed f_B values for each observation from the 25-35 solar zenith angle range were plotted versus the simultaneous AOT (500nm) in order to produce an estimate of the relative and absolute reductions in received total solar flux by smoke aerosol. The ratios of measured flux to expected flux for background aerosol conditions at each site are shown (with polynomial fit) in Figure 1a. Computed instantaneous shortfalls of received total irradiance were also plotted as a function of AOT (Figure 1b). The losses of solar radiation were found to be substantial, even at moderate AOT values (Table 1). Average irradiance reductions were 9% (at AOT 500: 0.5) and 37% (AOT 500: 3.0) at the Brazilian sites. Examination of absolute irradiance shortfalls (relative to expected values for background conditions) for the selected solar zenith angles (mean: 31 degrees) indicates that these f_B values correspond to absolute losses of 81 W/m² and 337 W/m², respectively.

For the Zambia data, the losses were comparatively greater than that observed at the Brazilian sites due to a lower typical effective SSA. Although the measured AOT (500nm) values did not exceed 1.8 at any of these sites, the average computed f_B was found to be 66% for these maximum AOT conditions, which indicates a shortfall of approximately 328 W/m² for the observed solar zenith angles (mean: 30 degrees). At an AOT of 1.0, the reduction at the African sites averages 65 W/m² greater than that observed at the Brazilian sites.

The variation in aerosol attenuation of flux between the Brazilian and Zambian measurements can be attributed to the different composition of fire source materials and their associated type of combustion. The African sites experience smoke originating primarily from the combustion of savanna grasses which have been observed to typically exhibit lower SSA values (more incomplete flaming phase combustion) than those produced by forest biomass combustion such as predominates in the Amazon region where smoldering phase combustion is more common [Eck et al., 2001].

The single scattering albedos retrieved using the pyranometer measurements were generally similar at the 2 Brazilian sites, perhaps due to the common nature of the biomass source (forest) and the prevalent wind patterns of the season that routinely transports smoke great distances in a westerly direction along the site transect. The average effective SSA was found to be 0.86 ± 0.04 at Alta Floresta and 0.87 ± 0.03 at Abracos Hill. As would be expected based on the greater flux reductions at Mongu, the effective SSA estimates here were lower, averaging 0.79 ± 0.03 . Single scattering albedos are typically lower for flaming phase combustion (which produces more black carbon) such as Mongu grass fires than for the smoldering phase conditions more commonly observed in the forest-source fires influencing Alta Floresta and Abracos Hill.

With the assumption of a wavelength-independent imaginary refractive index, the n_i can be estimated for each site that would be representative of the average effective SSA observed. The Brazilian sites indicated similar values (Alta Floresta: $n_i = 0.025$; Abracos Hill: $n_i = 0.024$) while the average imaginary refractive index at Mongu was evaluated equal 0.041 for its typical effective SSA. Figure 2 demonstrates the SSA wavelength dependence utilized by the 6S model (AOT: 1.0) for an assumed refractive index equal to the average n_i estimated for the location.

Concluding Remarks

This study has quantified substantial reductions in total solar flux produced by biomass-burning aerosols in Brazil and Zambia. Specifically, total solar flux reduction by smoke was estimated to be approximately -145 W/m² for a unit AOT (500nm) at the southern Amazonian sites and -210 W/m² in southern Africa. Instantaneous reductions observed in Brazil ranged from 9-37% (corresponding to an AOT range of 0.5 to 3.0) relative to the values expected for background aerosol conditions.

A similar, more extensive analysis of smoke aerosol attenuation in the visible spectral region has been completed based on the Brazilian sites, and has been submitted for inclusion in a

forthcoming LBA special issue of the Journal of Geophysical Research.

Acknowledgments. We thank the site managers responsible for maintaining the instrumentation suites and ensuring continuous, high quality data sets. These colleagues include Edilson Bernardino de Andrade (Alta Floresta), Rosivaldo Leles da Silva and Fabricio Berton Zanchi (Abracos Hill), and Mukufute Mukulabai. (Mongu), Stanley Shakalima (Zambezi), Overseas Mwangase (Ndola)

References

- Ackerman, A.S., O.B. Toon, D.E. Stevens, A.J. Heymsfield, V. Ramanathan, and E.J. Welton, Reduction of tropical cloudiness by soot, *Science*, 288, 1042-1047, 2000.
- Bergstrom, R.W., P.B. Russell and P. Hignett, On the wavelength dependence of the absorption of black carbon particles: Predictions and results from the TARFOX experiment and implications for the aerosol single scattering albedo, *J. Atmo. Sci.*, in press, 2001.
- Dubovik O., and M.D. King, A flexible inversion algorithm for retrieval of aerosol optical properties from Sun and sky radiance measurements, *J. Geophys. Res.*, 105, D16, 20,673-20,696, 2000.
- Eck TF, B.N. Holben, I. Slutsker, and A. Setzer, Measurements of irradiance attenuation and estimation of aerosol single scattering albedo for biomass burning aerosols in Amazonia *J. Geophys. Res.*, 103, D24, 31,865-31,878, 1998.
- Eck TF, B.N. Holben, D.E. Ward, O. Dubovik, J.S. Reid, A. Smirnov, M.M. Mukelabai, N.C. Hsu, N.T. O'Neill, and I. Slutsker, Characterization of the optical properties of biomass burning aerosols in Zambia during the 1997 ZIBBEE field campaign, *J. Geophys. Res.*, 106, 3425-3448, 2001.
- Facchini M.C.; M. Mircea, S. Fuzzi, and R.J. Charlson, Cloud albedo enhancement by surface-active organic solutes in growing droplets, *Nature*, 401, 257-259, 1999.
- Hansen, J., M. Sato, and R. Ruedy, Radiative forcing and climate response, *J. Geophys. Res.*, 102, 6831-6864, 1997.
- Holben, B.N., T.F. Eck, I. Slutsker, D. Tanre, J.P. Buis, A. Setzer, E. Vermote, J.A. Reagan, Y.K. Kaufman, T. Nakajima, F. Lavenue, I. Jankowiak, and A. Smirnov, AERONET - A federated instrument network and data archive for aerosol characterization, *Remote Sens. Environ.*, 66, 1-16, 1998.
- Konzelmann, T., D.R. Cahoon, and C.H. Whitlock, Impact of biomass burning in equatorial Africa on the downward surface shortwave irradiance: Observations versus calculations, *J. Geophys. Res.*, 104, D17, 22,833-22,844, 1996.
- Pereira E.B., FR Martins, and S.L. Abreu, Biomass burning controlled modulation of the solar radiation in Brazil, *Adv. Space Res.*, 24, Iss 7, 971-975, 1999.
- Smirnov A, Holben BN, Eck TF, O. Dubovik, I. Slutsker, Cloud-screening and quality control algorithms for the AERONET database, *Remote Sens. Environ.*, 73, 3, 337-349, 2000.
- Toon, O.B., Modeling aerosol properties and climatic effects, Ch. 11 in *Aerosol Forcing of Climate*, R.J. Charlson and J. Heintzenberg, ed., John Wiley and Sons, Chichester, England, 197-213, 1995.
- Vermote, E.F., D. Tanre, J.L. Deuze, M. Herman, and J.J. Morcrette, Second simulation of the satellite signal in the solar spectrum, 6S: An overview, *IEEE Trans. Geosci. and Remote Sens.*, 35, 675-686, 1997.
- Wild, M., Discrepancies between model-calculated and observed shortwave atmospheric absorption in areas with high aerosol loadings, *J. Geophys. Res.*, 104, D22, 27,361-27,371, 1999.